

Tapped Inductor Based Z-H Buck-Boost Converter

Hamideh Feyzi¹, Ebrahim Babaei¹, *Senior Member, IEEE*, Reza Gholizadeh-Roshanagh², Vida Ranjbarizad¹

¹Faculty of Electrical and Computer Engineering, University of Tabriz, Tabriz, Iran
h.feyzi92@ms.tabrizu.ac.ir; e-babaei@tabrizu.ac.ir; vidaranjbarizad@yahoo.com
²Young Researchers and Elite Club, Ahar Branch, Islamic Azad University, Ahar, Iran
rgr.elec@gmail.com

Abstract

In this paper, a new topology of Z-source converter based on tapped inductor is proposed. The proposed converter has two buck-boost and boost operating zones. Voltage boost factor of the proposed topology is adjusted by changing the turns ratio of the inductors. In the proposed converter, the shoot-through switching state and the front-end diode of the impedance network are eliminated. Other advantages of the proposed topology are buck and boost capability and elimination of the output filter. This topology can be utilized in dc-dc, ac-dc, dc-ac, and ac-ac conversions. In this paper, the operating principles of the proposed structure in dc-dc conversion are given in details. In order to reconfirm the results of the mathematical calculations, the simulation results are presented.

Keywords—Z-H buck-boost converter, Tapped inductor, Z-source converter.

1. Introduction

The conventional voltage source inverter, irrespective of its simple topology and control, has some disadvantages like unable to boost voltage and unprotected against shoot-through (ST) switching state. In order to overcome these disadvantages, in some applications, two-stage converter is utilized, in which, a dc-dc converter is used to increase the voltage gain before the inverter. Another solution is the use of Z-source inverter, which due to having ST switching state and being able to increase (decrease) voltage in one stage, has a great deal of applications. The conventional Z-source inverter [1] includes an X-shaped passive network, which has two ST and non-ST operating modes.

In comparison with the conventional voltage source inverter, the Z-source inverter, due to having ST state can increase or decrease the input voltage [2-3]. Besides, the Z-source inverter has good resistance against noise and electromagnetic interferences. These features make the Z-source inverter appropriate for different applications such as renewable energies [4, 5], adjustable speed drives [6], uninterruptible power supplies (UPS) [7], and etc. It should be mentioned that the front-end diode in Z-source structure makes some problems such as inappropriate operation in non-ST switching state (due to discrete nature of current) and not having ability of reverse current flow. Therefore, application of Z-source inverter is confined to some cases where there is no need to reverse flow of energy [1, 8]. Another kind of converters based on Z-source network have been presented in [9, 10], which can be used in dc-dc, ac-dc, dc-ac, and ac-ac conversions. These converters,

irrespective of ST-state's elimination, can increase or decrease the input voltage.

Conventional dc-dc boost converters dc-dc boost converters have low gains. So, a new converter with higher voltage gain is needed where the higher boost factor is required. In recent years, different structures have been presented to increase the voltage boost factor of power electronic converters [11, 12], where the main solution is to add new diodes, capacitors and inductors, which is not economical.

In [13-17], cells of tapped inductor, coupled inductor or transformer have been utilized to increase the voltage gain of the converters. In [16, 17], a coupled transformer and a capacitor in impedance network have been utilized to form a structure, which is called Trans-Z-source inverter. Trans-Z-source inverter has higher voltage gain than the conventional Z-source inverter, in which by changing the turns ratio of the transformer's inductors, appropriate voltage gain is obtained.

In this paper, a new topology of Z-H buck-boost inverter with tapped inductor is proposed, where by changing the turns ratio of the inductor, the voltage gain is controlled. Like the conventional Z-source inverter, there is no need for additional dc-dc converter and unlike it the ST switching state and the front-end diode are eliminated. One of the main features of the proposed structure is that with no change in its structure, it can be utilized in dc-dc, ac-dc, dc-ac, and ac-ac applications. Also, presence of mirrored tapped inductor makes it possible for the Z-H converter to be used for ac-ac applications. In some applications, where the higher voltage gain is required, the conventional Z-H buck-boost converter may be inappropriate, so the proposed buck-boost Z-H converter with tapped inductor of turn ratio as $\gamma_{TL} = N_2/N_1$ can be utilized.

In this paper, firstly, the operating principles of the proposed converter in dc-dc conversion are presented. Then, the voltage and current equations of the elements of the converter are obtained. Finally, in order to reconfirm the operation accuracy of the proposed converter, the simulation results are given by PSCAD/EMTDC software.

2. Proposed converter

The power circuit of the proposed converter is given in Fig. 1. It contains two tapped inductor cells and four bidirectional switches. The components of the first cell are L_{11} , L_{12} , D_1 and D_3 and of the second cell are L_{21} , L_{22} , D_2 and D_4 . In this structure, combination of two tapped inductor cells and two capacitors transfers energy from dc input to output dc bus. The voltages across diodes are higher than the switched inductor structure. In order to decrease the voltage stress, the values of inductors ($L_{11} + L_{12} = L_{21} + L_{22} = L_T$) and capacitors

($C_1 = C_2 = C$) are assumed to be equal. Also, it is assumed that $L_{11} = L_{21}$ and $L_{12} = L_{22}$. For tapped inductor cells, the turns ratio are considered as $\gamma_{TL} = N_2/N_1$ where N_1 is the number of turns of inductors L_{11} and L_{21} and N_2 is the number of turns of the inductors L_{12} and L_{22} . The following assumptions are also considered:

$$L_{11} = L_{21} = \left(\frac{N_1}{N_1 + N_2}\right)^2 L_T = \left(\frac{1}{1 + \gamma_{TL}}\right)^2 L_T \quad (1)$$

$$L_{12} = L_{22} = \left(\frac{N_2}{N_1 + N_2}\right)^2 L_T = \left(\frac{\gamma_{TL}}{1 + \gamma_{TL}}\right)^2 L_T \quad (2)$$

In ideal condition, the mutual inductance in each tapped inductor cell is defined as follows:

$$L_M = K \sqrt{L_{11} L_{22}} = \frac{\gamma_{TL}}{(1 + \gamma_{TL})^2} L_T \quad (3)$$

where K is coupling factor and is assumed to be equal to one (in ideal condition).

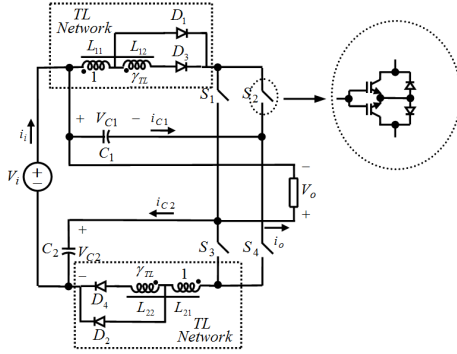


Fig. 1. Proposed converter

To simplify the analyses, all components of the converter are considered ideal. There are two operating zones for the proposed converter as $D = [0, 1/\gamma_{TL} + 2)$ and $D = (1/\gamma_{TL} + 2, 1]$, where in the first operating zone, the converter operates as a buck-boost converter and in the second operating zone, the converter operates as a boost converter. In order to control on and off states of the switches, a triangular carrier signal (A_c) is compared to a reference signal (A_r). Considering Fig. 2(a), in the first operating zone, $D = [0, 1/\gamma_{TL} + 2)$, when A_c is higher than A_r , the switches S_1 and S_4 are turned on, and when A_c is lower than A_r , the switches S_2 and S_3 are turned on. In this mode, the converter operates as a buck-boost converter. Also, considering Fig. 2(b), in the second operating zone, $D = (1/\gamma_{TL} + 2, 1]$, with the same control signals, the proposed converter operates as a boost converter. When the switches S_1 and S_4 are turned on, the switches S_2 and S_3 are turned off simultaneously, and vice versa. Duty cycle of the switches S_2 and S_3 is D and is defined as $D = T_0/T$, where T_0 is the time interval that these switches are on over a switching period of T .

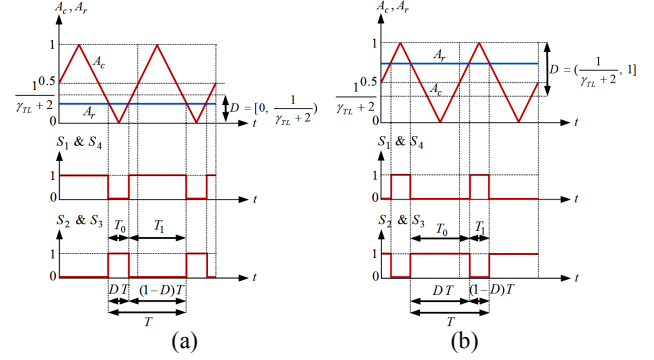


Fig. 2. Control signals; (a) $D = [0, 1/\gamma_{TL} + 2)$; (b) $D = (1/\gamma_{TL} + 2, 1]$

2.1. First Operating Mode (Time Interval T_0)

In this operating mode, the switches S_2 and S_3 and the diodes D_1 and D_2 are on and the switches S_1 and S_4 and the diodes D_3 and D_4 are off. Equivalent circuit of this mode is illustrated in Fig. 3(a). Assuming that the values of the inductors L_{11} and L_{21} are equal, and the capacitors C_1 and C_2 have equal values ($C_1 = C_2 = C$), the following equations can be obtained:

$$V_{C1} = V_{C2} = V_C \quad (4)$$

$$v_{L11} = v_{L21} = v_L \quad (5)$$

$$v_{D1} = v_{D2} = v_D \quad (6)$$

$$v_{D3} = v_{D4} = v_{D'} \quad (7)$$

where, V_C , v_L , v_D and $v_{D'}$ are the voltages across the capacitors C_1 and C_2 , the inductors L_{11} and L_{21} , the diodes D_1 and D_2 and the diodes D_3 and D_4 , respectively.

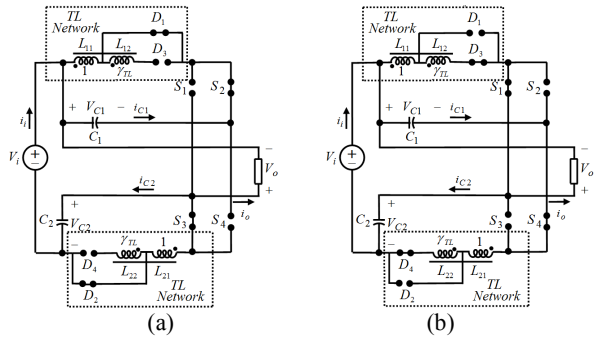


Fig. 3. Equivalent circuits; (a) time interval T_0 ; (b) time interval T_1

2.2. Second Operating Mode (Time Interval T_1)

Fig. 3(b) shows the equivalent circuit of the converter in the second operating mode. In this operating mode, the switches S_1

and S_4 and the diodes D_3 and D_4 are on and the switches S_2 and S_3 and the diodes D_1 and D_2 are off. So, in the upper tapped inductor cell, the inductors L_{11} and L_{12} and in the lower tapped inductor cell, the inductors L_{21} and L_{22} will be in series.

2.3. Voltage Gain Calculation

The average of voltage across capacitors (V_c) and the average output voltage (V_o) in both the operating zones, considering $T = T_0 + T_1$, can be obtained as:

$$\begin{aligned} V_c &= \frac{1-D}{1-D(\gamma_{TL}+2)} V_i > 0 \text{ for } D = [0, \frac{1}{\gamma_{TL}+2}) \\ &= \frac{1-D}{1-D(\gamma_{TL}+2)} V_i < 0 \text{ for } D = (\frac{1}{\gamma_{TL}+2}, 1] \end{aligned} \quad (8)$$

$$\begin{aligned} V_o &= \frac{D(\gamma_{TL}+1)}{1-D(\gamma_{TL}+2)} V_i > 0 \text{ for } D = [0, \frac{1}{\gamma_{TL}+2}) \\ &= \frac{D(\gamma_{TL}+1)}{1-D(\gamma_{TL}+2)} V_i < 0 \text{ for } D = (\frac{1}{\gamma_{TL}+2}, 1] \end{aligned} \quad (9)$$

Considering (9), the buck-boost factor of the converter can be defined as:

$$\begin{aligned} B &= \frac{V_o}{V_i} = \frac{D(\gamma_{TL}+1)}{1-D(\gamma_{TL}+2)} \\ &\text{for } D = [0, \frac{1}{\gamma_{TL}+2}) \text{ \& } D = (\frac{1}{\gamma_{TL}+2}, 1] \end{aligned} \quad (10)$$

According to the above equation, in the first operating zone, $D = [0, 1/\gamma_{TL}+2)$, the voltage gain has the values of $0 \leq B \leq 1$ (buck operation) and $1 \leq B \leq +\infty$ (boost operation), and in the second operating zone, $D = (1/\gamma_{TL}+2, 1]$, the voltage gain has just the values of $-\infty < B \leq -1$ (boost operation).

Considering (1)-(10), the voltage gain and the proportion of the voltage stress across capacitors to the input voltage with respect to the duty cycle under different turn ratios of tapped inductor for the two buck-boost and boost operating zones are illustrated in Fig. 4. From Fig. 4 it can be observed that:

- The duty cycle is divided into two operating zones, as $D = [0, 1/\gamma_{TL}+2)$ and $D = (1/\gamma_{TL}+2, 1]$, where in the first operating zone, the output voltage is positive and in the second one, the output voltage is negative.
- The voltage stresses across capacitors are different in the two operating zones.
- Minimum value of the voltage stress in the second operating zone is zero. So, in this operating zone the voltage stress across capacitors has lower value.

The voltages across the inductors and diodes in the time intervals T_0 and T_1 can be obtained as:

$$\begin{aligned} v_{L,T_0} &= V_{D',T_0} = \frac{1-D}{1-D(\gamma_{TL}+2)} V_i > 0 \text{ for } D = [0, \frac{1}{\gamma_{TL}+2}) \\ &= \frac{1-D}{1-D(\gamma_{TL}+2)} V_i < 0 \text{ for } D = (\frac{1}{\gamma_{TL}+2}, 1] \end{aligned} \quad (11)$$

$$\begin{aligned} v_{L,T_1} &= -\frac{D}{1-D(\gamma_{TL}+2)} V_i > 0 \text{ for } D = [0, \frac{1}{\gamma_{TL}+2}) \\ &= -\frac{D}{1-D(\gamma_{TL}+2)} V_i < 0 \text{ for } D = (\frac{1}{\gamma_{TL}+2}, 1] \end{aligned} \quad (12)$$

$$V_{D,T_0} = V_{D',T_1} = 0 \quad (13)$$

$$\begin{aligned} V_{D,T_1} &= \left(\frac{\gamma_{TL}D}{1-D(\gamma_{TL}+2)} \right) V_i > 0 \text{ for } D = [0, \frac{1}{\gamma_{TL}+2}) \\ &= \left(\frac{\gamma_{TL}D}{1-D(\gamma_{TL}+2)} \right) V_i < 0 \text{ for } D = (\frac{1}{\gamma_{TL}+2}, 1] \end{aligned} \quad (14)$$

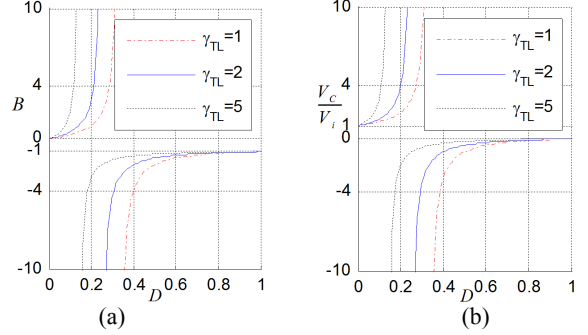


Fig. 4. Variations versus duty cycle under different turns ratio of tapped inductors; (a) voltage gain; (b) proportion of voltage stress across capacitors to the input voltage.

3. Extraction of the equations of currents

3.1. First Operating Mode (Time Interval T_0)

Considering v_L from (5) and by replacing $t = T_0 = DT$, the maximum current flowing through inductors L_{11} and L_{21} ($I_{2,L11}, I_{2,L21}$), at the end of the time interval T_0 , can be obtained as follows:

$$i_{L11,T_0} \Big|_{t=T_0=DT} = I_{2,L11} = \frac{V_c}{L_{11}} DT + I_{1,L11} \quad (15)$$

$$i_{L21,T_0} \Big|_{t=T_0=DT} = I_{2,L21} = \frac{V_c}{L_{21}} DT + I_{1,L21} \quad (16)$$

where $I_{1,L11}$ and $I_{1,L21}$ are initial values of currents flowing through the inductors L_{11} and L_{21} , in the time interval T_0 , respectively.

During the time interval T_0 , to have increasing state for the instantaneous currents flowing through the inductors L_{11} and L_{21} in the first operating zone and decreasing state in the second operating zone, the following conditions must be satisfied:

$$\frac{di_{L,T_0}}{dt} > 0 > 0 \text{ \& } V_c > 0 \text{ for } D = [0, \frac{1}{\gamma_{TL}+2}) \quad (17)$$

$$\frac{di_{L,T_0}}{dt} < 0 \text{ \& } V_c < 0 \text{ for } D = (\frac{1}{\gamma_{TL}+2}, 1] \quad (18)$$

Assuming that the output load is pure resistive, the instantaneous current flowing through the load will be equal to

the average current flowing through the load ($I_{o,av}$), in both operating zones and in both time intervals T_0 and T_1 . So, this results in:

$$i_{o,T0} = i_{o,T1} = I_{o,av} = \frac{V_o}{R} \quad (19)$$

3.2. Second Operating Mode (Time Interval T_1)

Like the first operating mode, by replacing $t = T_1 = (1-D)T$, the currents flowing through the inductors L_{11} and L_{21} , at the end of the time interval T_1 can be obtained as follows:

$$i_{L_{11},T1} \Big|_{t=T_1=(1-D)T} = I_{4,L_{11}} = \frac{V_i - V_C}{(\gamma_{TL} + 1)L_{11}}(1-D)T + I_{3,L_{11}} \quad (20)$$

$$i_{L_{21},T1} \Big|_{t=T_1=(1-D)T} = I_{4,L_{21}} = \frac{V_i - V_C}{(\gamma_{TL} + 1)L_{21}}(1-D)T + I_{3,L_{21}} \quad (21)$$

where $I_{3,L_{11}}$ and $I_{3,L_{21}}$ are the initial currents of the inductors L_{11} and L_{21} , in the time interval T_1 , respectively.

During the time interval T_1 , to have decreasing state for the instantaneous currents flowing through the inductors L_{11} and L_{21} in the first operating zone and increasing state in the second operating zone, the following conditions must be satisfied:

$$\frac{di_{L,T1}}{dt} < 0 \ \& \ (V_i < V_C) \ \text{for} \ D = [0, \frac{1}{\gamma_{TL} + 2}) \quad (22)$$

$$\frac{di_{L,T1}}{dt} > 0 \ \& \ (V_i > V_C) \ \text{for} \ D = (\frac{1}{\gamma_{TL} + 2}, 1] \quad (23)$$

According to (22) and (23), to transfer energy from input to output, in the first operating zone the value of voltage across the capacitors must be positive and be higher than input voltage, and in the second operating zone the value of voltage across the capacitors must be negative and be lower than the input voltage. The waveforms of the voltages and currents of the proposed converter in the operating zone $D = [0, 1/\gamma_{TL} + 2)$ and in the boost mode are illustrated in Fig. 5.

4. SIMULATION RESULTS

In order to reconfirm the correct operation and accuracy of the proposed converter, the simulations results by using PSCAD/EMTDC software are presented. The used parameters in simulated converter are given in Table 1. Fig. 6 shows the simulation results of the first operating zone $D = [0, 1/\gamma_{TL} + 2)$ and for the voltage gains of $B = 0.54$ and $B = 6$.

Table 1. Used parameters

f	R	$C_1 = C_2$	$L_{11} = L_{21}$	V_i	Duty Cycle	
25 kHz	5 Ω	50 μF	600 μH	20V	$D = 0.15$	Buck
	200 Ω				$D = 0.3$	Boost

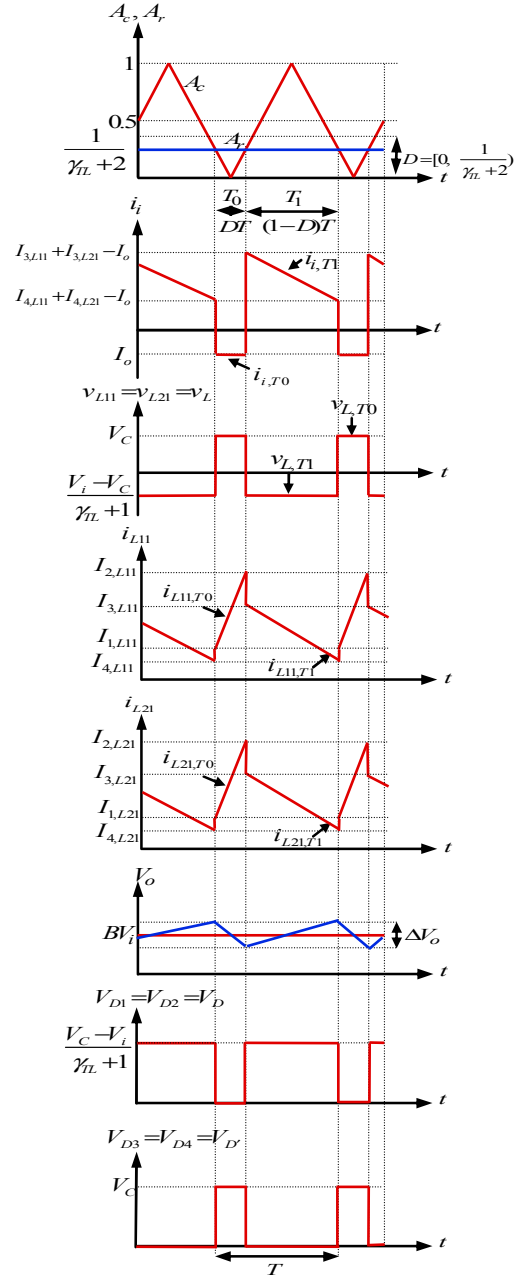


Fig. 5. Waveforms of voltages and currents of the proposed converter in the operating zone $D = [0, 1/\gamma_{TL} + 2)$ and in the boost mode.

From (8) and (9), the values of the output voltage of the converter and the voltage across the capacitors in both the time intervals T_0 and T_1 can be obtained as follows:

$$V_o = \frac{D(\gamma_{TL} + 1)}{1 - D(\gamma_{TL} + 2)} V_i = \frac{0.3 \times 2}{1 - 0.3 \times 3} \times 20 = 120V$$

$$V_C = \frac{1 - D}{1 - D(\gamma_{TL} + 2)} V_i = \frac{1 - 0.3}{1 - 0.3 \times 3} \times 20 = 140V$$

From (11)-(14), the values of the voltages across inductors and diodes, in the time intervals T_0 and T_1 are obtained as

$v_{L,T0} = V_{D'T0} = 140V$ and $v_{L,T1} = -60V$, $V_{D,T0} = V_{D'T1} = 0$ and $V_{D,T1} = 60V$, respectively.

Simulation results in Fig. 6 reconfirm the values obtained through mathematical calculations.

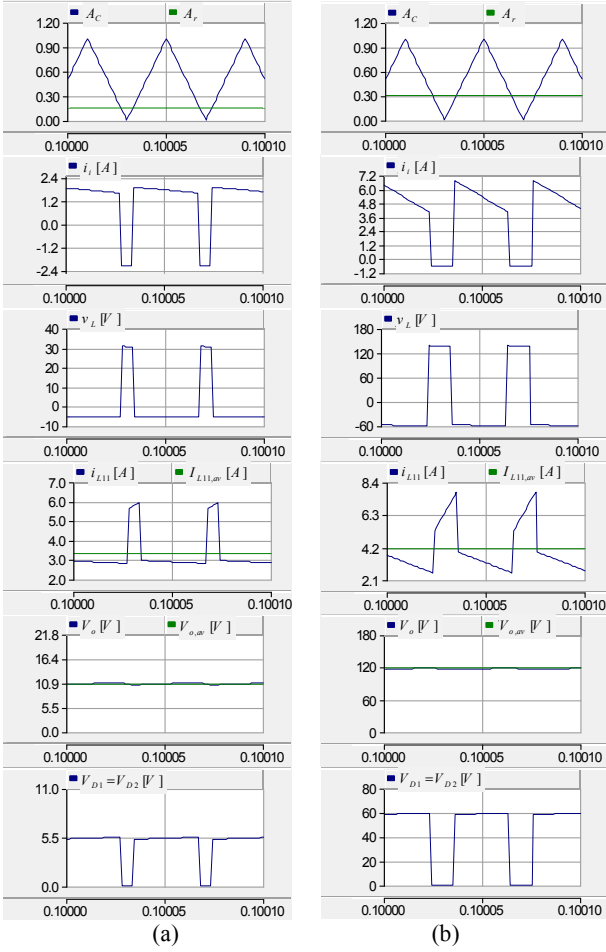


Fig. 6. Simulation results of the proposed converter in the first operating zone as $D = [0, \frac{1}{\gamma_{TL} + 2})$; (a) buck mode for $B = 0.54$ and $D = 0.15$; (b) boost mode for $B = 6$ and $D = 0.3$.

5. CONCLUSION

In this paper, a new topology of Z-H buck-boost converter with tapped inductor was proposed. A complete analysis of operating principles of the proposed converter was presented in the buck-boost and boost operations. In the proposed structure, by changing the turns ratio of the tapped inductor cell, the voltage gain is adjusted. In this structure, without changing the number of inductors, and by varying the turn ratio and the duty cycle, the desired voltage gain is obtained. Also, in order to reconfirm the accuracy of the proposed converter, the simulation results were given for both the buck and boost modes in the PSCAD/EMTDC software.

REFERENCES

- [1] F.Z. Peng, "Z-source inverter," *IEEE Trans. Ind. Appl.*, vol. 39, no. 2, pp. 504-510, Mar./Apr. 2003.
- [2] E. Babaei, E. Shokati Asl, and M. Hasan Babayi, "Steady-state and small-signal analysis of high voltage gain half-bridge switched-boost inverter," *IEEE Trans. Ind. Electron.*, vol. 63, no. 6, pp. 3546-3553, June 2016.
- [3] L. Pan, "L-Z-source inverter," *IEEE Trans. Power Electron.*, vol. 29, no. 12, pp. 6534-6543, Dec. 2014.
- [4] Y. Huang, M. Shen, F.Z. Peng, and J. Wang, "Z-source inverter for residential photovoltaic systems," *IEEE Trans. Power Electron.*, vol. 21, no. 6, pp. 1776-1782, Nov. 2006.
- [5] E. Babaei, E. Shokati Asl, M. Hasan Babayi, and S. Laali, "Developed embedded switched-Z-source inverter," *IET Power Electron.*, vol. 9, no. 9, pp. 1828-1841, July 2016.
- [6] F.Z. Peng, "Z-source inverter for adjustable speed drives," *IEEE Power Electron. Lett.*, vol. 1, no. 2, pp. 33-35, Jun. 2003.
- [7] Z.J. Zhou, X. Zhang, P. Xu, and W.X. Shen, "Single-phase uninterruptible power supply based on Z-source inverter," *IEEE Trans. Ind. Electron.*, vol. 55, no. 8, pp. 2997-3004, Aug. 2008.
- [8] R. Strzelecki and N. Strzelecka, "Simulation investigation of the Z-source NPC inverter," *Doctoral school of energy- and geo-technology, Kuressaare, Estonia*, Jan. 2007, pp. 213-218.
- [9] F. Zhang, F.Z. Peng, and Z. Qian, "Z-H converter," in *Proc. PESC*, 2008, Rhodes, pp. 1004-1007.
- [10] T. Ahmadzadeh, and E. Babaei, "Z-H buck converter: Analysis and simulation," in *Proc. PEDSTC*, 2015, Iran, pp. 436-441.
- [11] D. Li, F. Gao, P.C. Loh, M. Zhu, and F. Blaabjerg, "Hybrid-source impedance networks: Layouts and generalized cascading concepts," *IEEE Trans. Power Electron.*, vol. 26, no. 7, pp. 2028-2040, Jul. 2011.
- [12] M. Zhu, K. Yu, and F.L. Luo, "Switched inductor Z-source inverter," *IEEE Trans. Power Electron.*, vol. 25, no. 8, pp. 2150-2158, Aug. 2010.
- [13] M. Zhu, D. Li, P.C. Loh, and F. Blaabjerg, "Tapped-inductor Z-source inverters with enhanced voltage boost inversion abilities," in *Proc. IEEE Int. Conf. Sustainable Energy Technol.*, 2010, pp. 1-6.
- [14] M. Adamowicz, "LCCT-Z-source inverters," in *Proc. Int. Conf. Environ. Elect. Eng.*, 2011, pp. 1-6.
- [15] E. Babaei, M. Hasan Babayi, E. Shokati Asl, and S. Laali, "A new topology for Z-source inverter based on switched-inductor and boost Z-source inverter," *Journal of Operation and Automation in Power Engineering*, vol. 3, no. 2, pp. 167-184, Sep. 2015.
- [16] R. Strzelecki, M. Adamowicz, N. Strzelecka, and W. Bury, "New type T-source inverter," in *Proc. Compat. Power Electron.*, 2009, pp. 191-195.
- [17] W. Qian, F.Z. Peng, and H. Cha, "Trans-Z-source inverters," *IEEE Trans. Power Electron.*, vol. 26, no. 12, pp. 3453-3463, Dec. 2011.